iScience

CellPress
OPEN ACCESS

Article

I_{KACh} is constitutively active via PKC epsilon in aging mediated atrial fibrillation

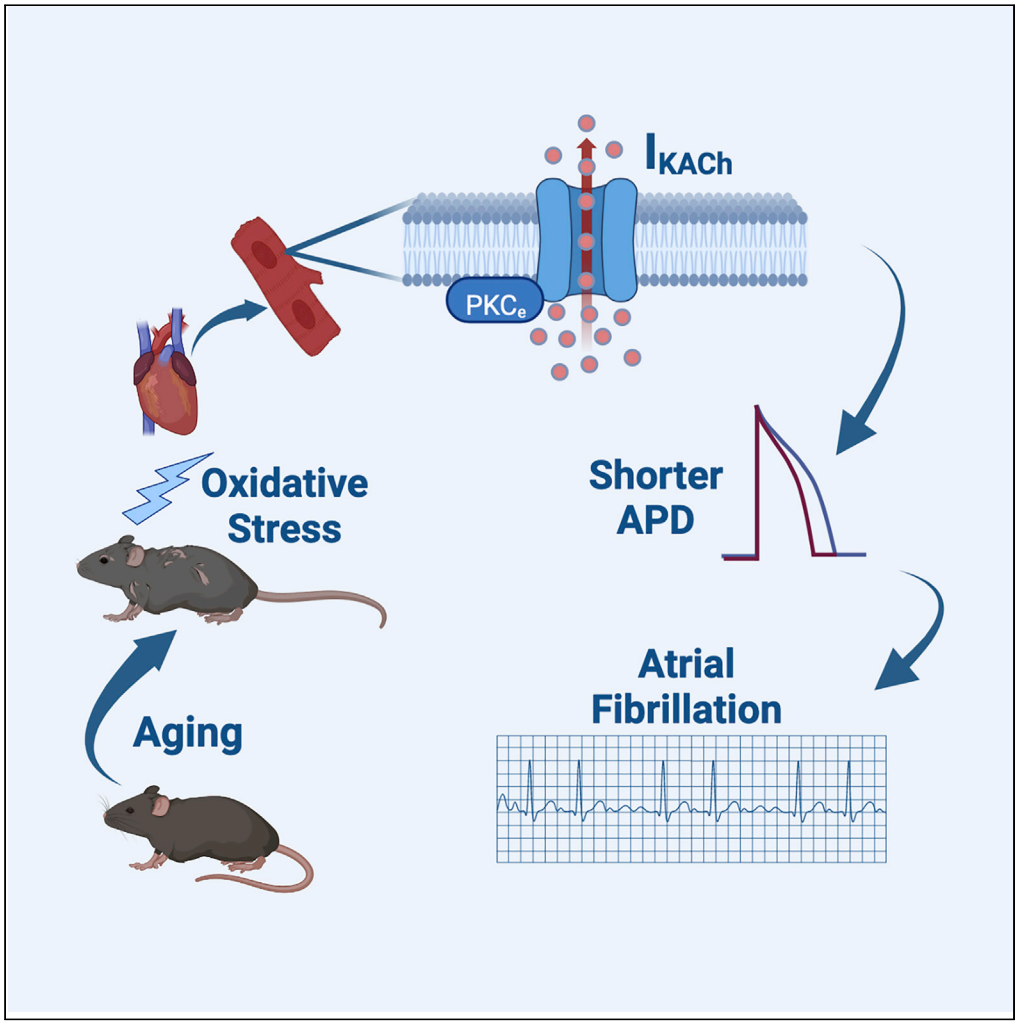

Mengmeng Chang, Kirin D. Gada, Bojjibabu Chidipi, ..., Diomedes E. Logothetis, Jenna Oberstaller, Sami F. Noujaim

snoujaim@usf.edu

Highlights

Atrial fibrillation (AF) is highly prevalent in aging and is a major cause of stroke

A potassium current (I_{KACh}) is aberrantly active in atrial myocytes from aged hearts

Knocking out PKCε prevents the development of this aberrant current

Blocking I_{KACh} or knocking out PKCε abrogates the effects of aging on AF

Chang et al., iScience 25, 105442
November 18, 2022
https://doi.org/10.1016/j.isci.2022.105442

iScience

CellPress
OPEN ACCESS

Article

I_{KACh} is constitutively active via PKC epsilon in aging mediated atrial fibrillation

Mengmeng Chang,[1] Kirin D. Gada,[2] Bojjibabu Chidipi,[1] Athanasios Tsalatsanis,[3] Justin Gibbons,[4] Elizabeth Remily-Wood,[5] Diomedes E. Logothetis,[2] Jenna Oberstaller,[4] and Sami F. Noujaim[1,6,*]

SUMMARY

Atrial fibrillation (AF), the most common abnormal heart rhythm, is a major cause for stroke. Aging is a significant risk factor for AF; however, specific ionic pathways that can elucidate how aging leads to AF remain elusive. We used young and old wild-type and PKC epsilon- (PKCϵ) knockout mice, whole animal, and cellular electrophysiology, as well as whole heart, and cellular imaging to investigate how aging leads to the aberrant functioning of a potassium current, and consequently to AF facilitation. Our experiments showed that knocking out PKCϵ abrogates the effects of aging on AF by preventing the development of a constitutively active acetylcholine sensitive inward rectifier potassium current (I_{KACh}). Moreover, blocking this abnormal current in the old heart reduces AF inducibility. Our studies demonstrate that in the aging heart, I_{KACh} is constitutively active in a PKCϵ-dependent manner, contributing to the perpetuation of AF.

INTRODUCTION

Atrial fibrillation (AF) is the most common arrhythmia in clinical practice[1] and its management has become a global challenge.[2] AF is characterized by rapid and irregular electrical and mechanical activation of the atria. AF is a major risk factor for stroke, thromboembolism, heart failure, and myocardial infarction.[3–13] Consequently, AF constitutes a major public health burden.[14]

Epidemiological studies have shown that the natural history of AF is progressive,[15,16] and that aging is the single greatest risk factor for AF, with each decade of life after the age of 40 conferring up to a 2-fold higher risk.[17] Unfortunately, the underlying mechanisms of aging-mediated AF are not well understood, and the current pharmacological and more invasive therapeutic interventions have numerous limitations and remain inadequate in treating this disease.[18]

Cardiac aging is a complex process, characterized by a gradual increase in cardiac remodeling,[19] as well as increased generation and/or accumulation of reactive oxygen species (ROS).[20] For instance, during aging, changes in atrial structure and function take place, including changes in atrial refractoriness, atrial conduction, aberrant impulse formation, and fibrosis.[21] In addition, oxidative stress has been proposed to play a role in the pathogenesis of AF[22] where increased levels of myocardial ROS such as superoxide (O_2^-) and hydrogen peroxide (H_2O_2) have been found to be associated with AF.[23–26] These factors constitute the appropriate electrophysiological and anatomical substrates conducive for the initiation and perpetuation of AF.

Electrical remodeling promotes AF by abbreviating atrial refractoriness. This involves shortening of the action potential duration (APD), in part, via increased inwardly rectifying potassium currents such as the background current I_{K1} and the constitutively active form of the acetylcholine-dependent inwardly rectifying potassium current (I_{KACh}).[27–31] Cardiac I_{KACh} is a heterotetramer of G protein-regulated inwardly rectifying potassium channel subunits, known as Kir3.1 and Kir3.4.[32–34] In normal physiology, I_{KACh} is activated by vagally released acetylcholine (ACh) which in turn activates type 2 muscarinic (M2) receptors. This results in the dissociation of the α and the βγ subunits of the inhibitory Gi protein and the subsequent activation of I_{KACh} because of the direct interaction of the βγ-subunits with the I_{KACh} channel proteins.[35–37] The I_{KACh} gating is tightly regulated as this ionic current is important in mediating the chronotropic parasympathetic effects resulting in the decrease of heart rate.[38,39] However, in AF I_{KACh} is constitutively

[1]Department of Molecular Pharmacology and Physiology, Morsani College of Medicine, University of South Florida, Tampa, FL 33612, USA

[2]Department of Pharmaceutical Sciences, School of Pharmacy and Pharmaceutical Science, Bouvé College of Health Sciences, Center for Drug Discovery, Northeastern University, Boston, MA 02115, USA

[3]College of Medicine Office of Research, Morsani College of Medicine, University of South Florida, Tampa, FL 33612, USA

[4]Center for Global Health and Infectious Diseases Research and USF Genomics Program, College of Public Health, University of South Florida, Tampa, FL 33612, USA

[5]Department of Molecular Medicine, Morsani College of Medicine, University of South Florida, Tampa, FL 33612, USA

[6]Lead contact

*Correspondence: snoujaim@usf.edu

https://doi.org/10.1016/j.isci.2022.105442

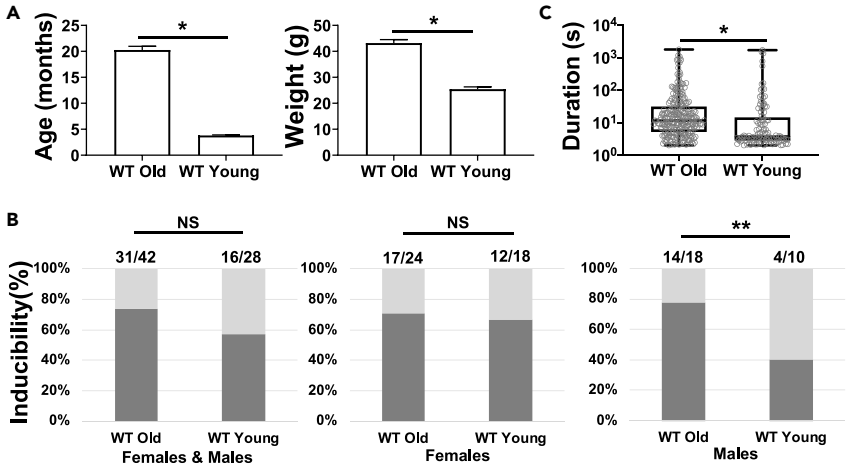

Figure 1. Aging increases AF inducibility and duration

(A) Age (left) and weight (right) are significantly different between WT old and WT young mice.

(B) AF inducibility comparison between WT old (N = 42) and WT young (N = 28) mice. (Left panel) AF inducibility was not different between WT old (31 out of 42 mice) comparable to WT young mice (16 out of 28), of both genders. (Middle) No significant difference of AF inducibility was found between WT old female mice (17 out of 24) and WT young female mice (12out of 18). (Right) AF inducibility of WT old male mice (14 out of 18) is notably higher than WT young male mice (4 out of 10). **p<0.01, Chi-square test.

(C) AF duration comparison between WT old (N = 42) and WT young (N = 28) mice. Induced AF duration in WT old mice is longer than in WT young mice. *p<0.01, linear mixed model adjusted for gender. Bar graphs: mean ± SEM Boxplots: median, 25th and 75th percentiles, minimum and maximum.

active, independent of parasympathetic signaling. This constitutively active current subsequently works as a background current, promoting atrial APD abbreviation, and shortening of the refractory period, which contributes to the initiation and perpetuation of AF.[27,29,40–43]

It is thought that a specific isoform of protein kinase C, PKCε, is active and plays a role in the electrical remodeling of the fibrillating atria.[44] More specifically, animal and human studies have postulated that the activated PKCε in chronic AF may be responsible for I_{KACh} constitutive activity.[40] PKC activation involves translocation of the protein from the cytosolic autoinhibited latent form to the membrane associated active form.[45,46] Of interest, oxidative stress has been demonstrated to lead to PKCε activation,[47] and it was recently shown by Yoo and colleagues[48] that oxidative stress because of mitochondrial ROS and NOX2 underlies PKCε activation in canine atria with pacing induced AF. They further showed that NOX2 knockdown suppressed ROS production and therefore PKCε activation.

Presently, it is not known whether the PKCε/I_{KACh} axis plays a role in aging-mediated AF. Therefore, in this study, we directly examined if the PKCε/I_{KACh} interplay is important in the mechanism of aging-mediated AF. We set out to test the hypothesis that in the aging heart, I_{KACh} is constitutively active via a PKCε mechanism, leading to generation of AF.

RESULTS

PKCε contributes to AF initiation and perpetuation in the old heart

To investigate the role of aging in AF initiation and perpetuation, we conducted a set of *in vivo* electrophysiological studies with intracardiac programmed electrical stimulation in wild-type (WT) young and old mouse hearts. Figure 1A shows the significantly different age (left) and weight (right) of the old compared to the young WT mice. When both genders were considered, the inducibility of AF in old WT mice was not significantly different from that in young WT mice (Figure 1B left panel). Similarly, the inducibility of AF in female mice was not different between old and young WT animals (Figure 1B middle). However, AF inducibility was statistically higher in old WT compared to young WT male mice (Figure 1B right). The duration of induced AF adjusted for gender was significantly longer in old WT mice compared to young (Figure 1C), suggesting a gender specific difference in AF inducibility.

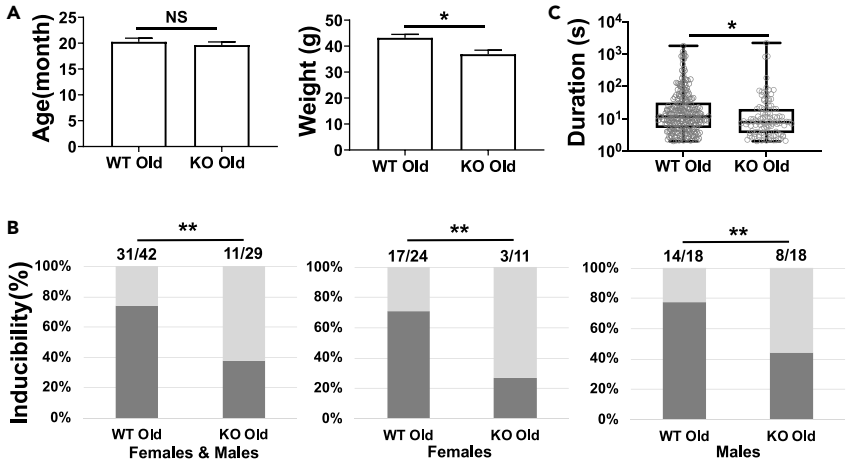

Figure 2. Knocking out PKCϵ abrogates the effects of aging on AF

(A) Age and weight comparison between WT old and KO old mice. (Left) Age of WT old and KO old mice are comparable. (Right) The weight of WT old is significantly heavier than KO old mice.

(B) AF inducibility comparison between WT old (N = 42) and KO old (N = 29) mice. (Left) AF inducibility in WT old mice (31 out of 42) is significantly higher than KO old mice (11 out of 29) of both genders. (Middle) AF inducibility in WT old female mice (17 out of 24) is significantly higher than in KO old female mice (3 out of 11). (Right) AF inducibility in WT old male mice (14 out of 18) is significantly higher than KO old male mice (8 out of 18). **p<0.01, Chi-square test.

(C) AF duration comparison between WT old (N = 42) and KO old (N = 29) mice. AF duration in WT old mice is longer than in KO old mice. *p<0.01, linear mixed model adjusted for gender. Bar graphs: mean ± SEM Boxplots: median, 25th and 75th percentiles, minimum and maximum.

To investigate the possible role of PKCε in AF initiation and perpetuation in the old heart, we assessed AF inducibility and duration in old PKCε knock-out (KO) versus old WT animals. The age of old WT and old KO animals was not different, but there was a difference in body weight (Figure 2A). AF inducibility was significantly reduced in old KO mice compared to old WT mice of both genders (Figure 2B). In addition, the duration of induced AF in the old KO mice was significantly shorter than that in the old WT mice (Figure 2C). Knocking out PKCε abrogated the effects of aging on AF inducibility and duration. These results suggest that PKCϵ plays an important role in the inducibility and stability of AF in the aging heart.

Constitutively active I_{KACh} is arrhythmogenic in the old heart

To investigate whether constitutively active I_{KACh} plays a role in aging-mediated AF, we assessed the *in vivo* inducibility and duration of AF in old WT mice after jugular vein administration of the I_{KACh} blocker tertiapinQ (TPQ). TPQ is a 21 amino acid synthetic peptide originally isolated from the European Honey bee venom. TPQ is atrial-selective in the heart, blocking I_{KACh} without affecting other inward rectifier potassium currents such as I_{K1} or I_{KATP}. However, in the kidney, TPQ blocks Kir1.1, a renal outer medullary potassium channel.[49,50] Moreover, TPQ prolongs the effective refractory period and terminates AF that is dependent on constitutively active I_{KACh}, or AF that is dependent on I_{KACh} activated with an M_2 agonist.[27,29,40–43] Here, TPQ administration significantly reduced the duration and the inducibility of AF in the old WT mice compared to saline vehicle control (Figure 3A), suggesting that I_{KACh} is constitutively active in the old heart. However, in KO old mice, TPQ did not affect AF duration and inducibility, indicating that I_{KACh} is not constitutively active in the atria of old KO mice (Figure 3B).

Subsequently, we used patch clamp in atrial myocytes isolated from WT and KO mice to further explore constitutively active I_{KACh} in the old atrial myocytes, and whether knocking out PKCε would abrogate the effects of aging on the development of constitutively active I_{KACh}. The background inwardly rectifying currents were measured in 50 mM $[K]_o$ before and after addition of 100 nM TPQ to the bath solution as previously reported[43] (Figure 4). In the young WT (Panel A), and young KO atrial myocytes (Panel B), TPQ did not affect the background currents, suggesting that I_{KACh} was not constitutively active. In the old WT atrial myocytes (Panel C), application of TPQ resulted in a significant decrease in the background current, indicating that I_{KACh} was constitutively active in the old heart, and that the constitutively active I_{KACh} works as a component of the background current in the old cardiomyocytes. In the old KO atrial myocytes (Panel

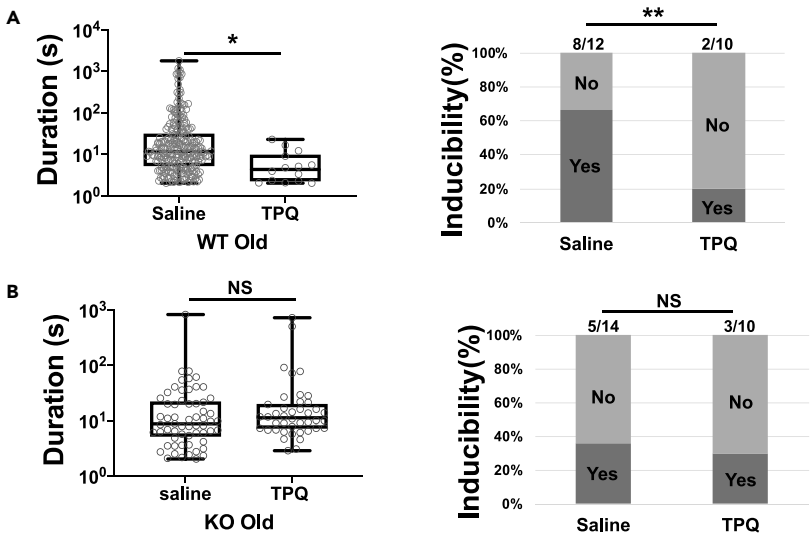

Figure 3. Blocking I_{KACh} with TPQ is antiarrhythmic in the old WT heart

(A) AF duration and inducibility in WT old mice injected with TPQ or Saline. Left: AF duration is reduced by TPQ in WT old mice. Right: AF inducibility is decreased by TPQ in WT old mice. N = 12 mice for saline and N = 10 mice for TPQ treatment. Box & whiskers, Min-Max.

(B) The effect of TPQ on AF duration and inducibility in KO old mice. Left: In KO old mice, AF duration is not changed by TPQ. Right: AF inducibility is not changed by TPQ in KO old mice. N = 14 mice for saline and N = 10 mice for TPQ treatment. N = 12 for saline and N = 10 for TPQ treatment. Boxplots: median, 25th and 75th percentiles, minimum and maximum. NS: not significant. *p<0.01, Mann Whitney Wilcoxon test.**p<0.01, Chi square test.

D), TPQ did not reduce significantly the background current, implying that knocking out PKCε diminishes the aging effect on constitutively active I_{KACh}. TPQ-sensitive, agonist-independent, constitutively active I_{KACh} was quantified at −140 mV and shown in the graph of Figure 4E. The constitutively active I_{KACh} was significantly larger in the old WT myocytes compared to young WT, young and old PKCε KO myocytes.

Knocking out PKCϵ prevents APD shortening in the old heart

To further investigate whether I_{KACh} was constitutively active in the old atria, we tested the effects of TPQ on the atrial action potential duration (APD) in the isolated Langendorff-perfused mouse heart in a PKCε-dependent manner using optical mapping. Our data indicate that 200 nM TPQ prolonged the APD in the old WT but not old PKCε KO hearts (Figure 5). Figure 5A is an APD map at 60% repolarization (APD_{60}) of the right atrium in an old WT (top) and and old KO (bottom) heart in control, and after TPQ treatment. TPQ caused an appreciable prolongation of the APD in the WT, but not in the KO hearts. Single-pixel optical tracings of voltage from the maps in Figure 5A show that TPQ prolonged APD in WT old but not in KO old hearts (Figures 5B and 5C). Figure 5D is a compilation of APD_{60} in 4 old WT and 4 old KO hearts. TPQ caused significant APD prolongation in WT, but not in KO. Additionally, at baseline control, the APD in WT hearts was significantly shorter than the baseline APD in KO hearts. This experiment shows that I_{KACh} is constitutively active in the old WT heart at the tissue level, in a PKCϵ-dependent manner.

Oxidative stress induces cell membrane translocation of PKCϵ, leading to increased I_{KACh}

Increased levels of myocardial ROS such as superoxide (O_2^-) and hydrogen peroxide (H_2O_2) have been found to be associated with AF.[23–26] Additionally, the ability of oxidative stress to recruit PKC isoforms to the cell surface has been shown.[45,51] To assess if H_2O_2 recruits PKCε to the cell surface, we used the catalytic domain of PKCε tagged with mCherry (mCherry-CRY2-mPKCεCAT-HA) in total internal reflection fluorescence microscopy (TIRFM) experiments. This technique allows imaging of fluorescent proteins localized to the cell membrane. Cells transfected with mCherry-CRY2-mPKCεCAT-HA were incubated with H_2O_2 and imaged at baseline and 5, 15, and 30 min after H_2O_2 treatment. mCherry was excited with a 561 nm, 'red' laser before and after H_2O_2 treatment (Figure 6A). These data, summarized in Figure 6B, show a significant increase in mCherry fluorescence at the cell surface after a 30-min incubation with

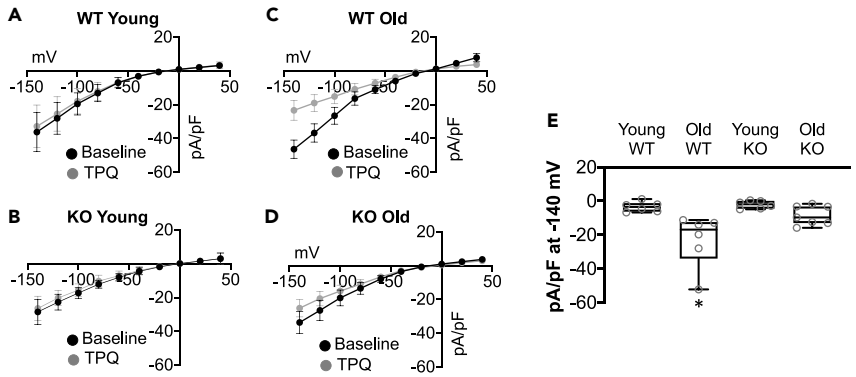

Figure 4. I_{KACh} is constitutively active in old WT atrial myocytes

(A) IV curves of the background current in young WT atrial myocytes before (black) and after 100 nM TPQ (gray), N = 2 mice, n = 6 cells.

(B) IV curves in young KO atrial myocytes before (black) and after TPQ (gray), N = 2 mice, n = 6 cells.

(C) IV curves in old WT atrial myocytes before (black) and after TPQ (gray), N = 2 mice, n = 6 cells.

(D) IV curves in old KO atrial myocytes before (black) and after TPQ (gray), N = 2 mice, n = 7 cells.

(E) Quantification of the TPQ sensitive, constitutively active I_{KACh} at −140 mV, and Shapiro-Wilk test confirmed normality of data. *p<0.05, one-way ANOVA with Bonferroni correction. IV curves: mean ± SEM Boxplots: median, 25th and 75th percentiles, minimum and maximum.

100 μM H_2O_2 compared to surface fluorescence at baseline, demonstrating that H_2O_2-mediated oxidative stress induced PKCε translocation to the cell surface.

To provide a mechanistic link between aging, PKCε and constitutively active I_{KACh}, we measured the basal I_{KACh} current in HEK cells stably transfected with Kir3.1 and Kir3.4, with PKCε knockdown, in the presence or absence of 100 μM H_2O_2, as a surrogate exposure to simulate oxidative stress associated with aging. The basal I_{KACh} current was recorded in 50 mM extracellular potassium. Figure 6C shows in representative I-V curves that 100 μM H_2O_2 for 1-h resulted in a larger I_{KACh} (red trace) compared to control (black). Silencing PKCε (green trace) prevented the increase of the current brought about by 100 μM H_2O_2. In Figure 6D, data were compiled showing that H_2O_2 significantly increased the maximum inward current, and silencing PKCε prevented this H_2O_2 induced increase in I_{KACh}.

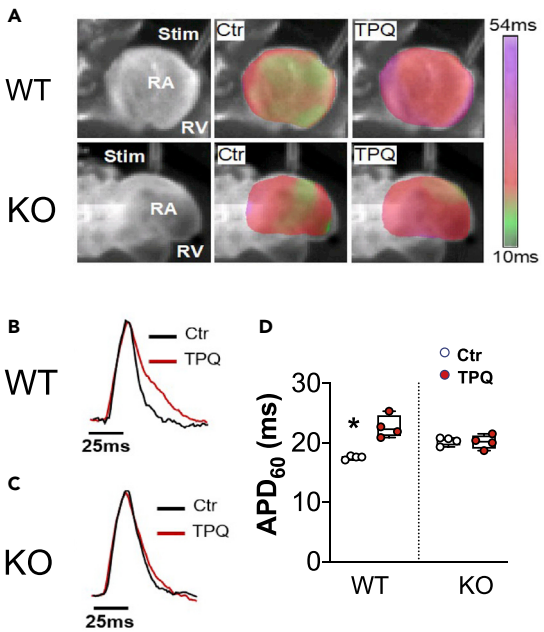

Figure 5. In optical mapping of Langendorff-perfused old WT and KO mouse hearts, bocking constitutively active I_{KACh} prolongs the APD in old WT hearts.

(A) APD_{60} maps of the right atria isolated from WT (top) and KO (bottom) hearts respectively, under control condition (middle) and after 200 nM TPQ application (right). 200 nM TPQ lead to appreciable APD prolongation in WT but not KO old mice.

(B and C) Single pixel voltage recordings showing longer APD after TPQ application (red) in WT (B), but in KO, TPQ did not prolong the APD (C).

(D) Plot of APD_{60} quantification, at control and after TPQ application showing TPQ significantly prolonged the APD in the WT heart (N = 4 hearts). Shapiro-Wilk test confirmed normality of data. *p<0.05, WT Ctr versus WT TPQ, and KO Ctr, and KO TPQ, One-way ANOVA with Bonferroni correction. Stim, stimulation; RA, right atria; RV, right ventricle; Ctr, control; TPQ, tertiapinQ.

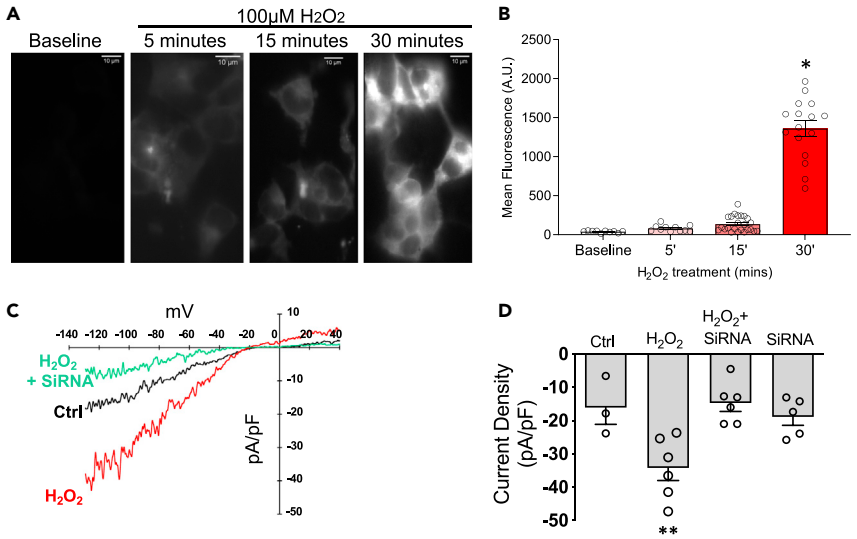

Figure 6. Oxidative stress results in increased I_{KACh} via translocation of PKCε

(A and B) Representative TIRFM images showing recruitment of mCherry-CRY2-mPKCεCAT-HA to the cell surface by 100 μM H_2O_2. Scale bar: 10 μm (B) Summary data showing cell surface localization of mCherry-CRY2-mPKCεCAT-HA at the cell surface following treatment with H_2O_2 (n = 10 cells for baseline, n = 12 cells for the 5 min, n = 24 cells for the 15 min, and n = 16 cells for the 30 min time points).

(C) IV curves of basal I_{KACh} (tertiapin sensitive current) control (black), H_2O_2 treated (red), and PKCε silenced and H_2O_2 treated (green), as measured in HEK293 cells stably expressing Kir3.1 and Kir3.4, and co-transfected with PKCε SiRNA and GFP.

(D) Quantification of maximum inward current. n = 3 cells for control, n = 6 cells for H_2O_2, n = 6 cells for H_2O_2+SiRNA, and n = 5 cells for SiRNA alone. Shapiro-Wilk test confirmed normality of data. *p<0.05, baseline versus 30 min H_2O_2, and **p<0.05, H_2O_2 versus all other conditions. One-way ANOVA with Bonferroni correction. Bar graphs: mean ± SEM.

Transcriptomic changes in old KO versus WT mouse atria

We conducted RNAseq on three old KO and three old WT mouse atrial samples in order to investigate whether knocking out PKCε resulted in transcriptomic changes of major ion channels that underlie the action potential, and thus could shed light on the reduced arrhythmogenesis in the old KO compared to old WT mice. Analysis revealed that out of the 8,631 genes detected above threshold, a total of 38 genes were differentially regulated, with 19 downregulated and 19 upregulated genes in the old KO compared to old WT mice (Tables S1 and S2). None of these differentially regulated genes were for sarcolemmal ion channels. The differentially expressed genes between KO and WT mice were then evaluated for gene ontology (GO) enrichment against all detected genes (Figure 7 and Table S3). There were 22 significantly upregulated and 9 significantly downregulated biological processes (Figure 7). Interestingly, biological processes related to regulation of fat cell differentiation, thermogenesis, and metabolic processes were enriched. This enrichment in transcriptomic programs that control metabolism and fat-cell development converge with our finding that body weight of KO old was significantly reduced compared to the WT old animals (Figure 2B), suggesting that a total knock out of PKCε may affect body weight through pathways relevant to metabolism and adipose tissue regulation. It should be mentioned that obesity is a risk factor for AF,[52] and thus the reduction in the body weight of KO mice might be a confounder that affects atrial arrhythmogenesis. Future studies in cardiac-specific PKCε knock out animals are required to address such confounders.

Proteomic differences in female versus male mouse atria

Since results suggested that there are sex-specific differences in the inducibility of AF (Figure 1), we explored in female versus male atrial samples from young WT animals the differentially abundant proteins that could be relevant to AF using proteomics approaches. In our samples, 3008 proteins were detected above threshold across all samples and were assessed for differential expression (Table S4). Of these, 55 proteins were significantly differentially abundant between the sexes, where 32 proteins were increased, and 23 were decreased in females compared to males (Table S5). Differentially regulated biological processes included pathways important for steroid processes, cardiac development, regeneration, immune response related pathways, and components of the gene regulatory apparatus including the mRNA splicing machinery (Figure 8; Table S6). These

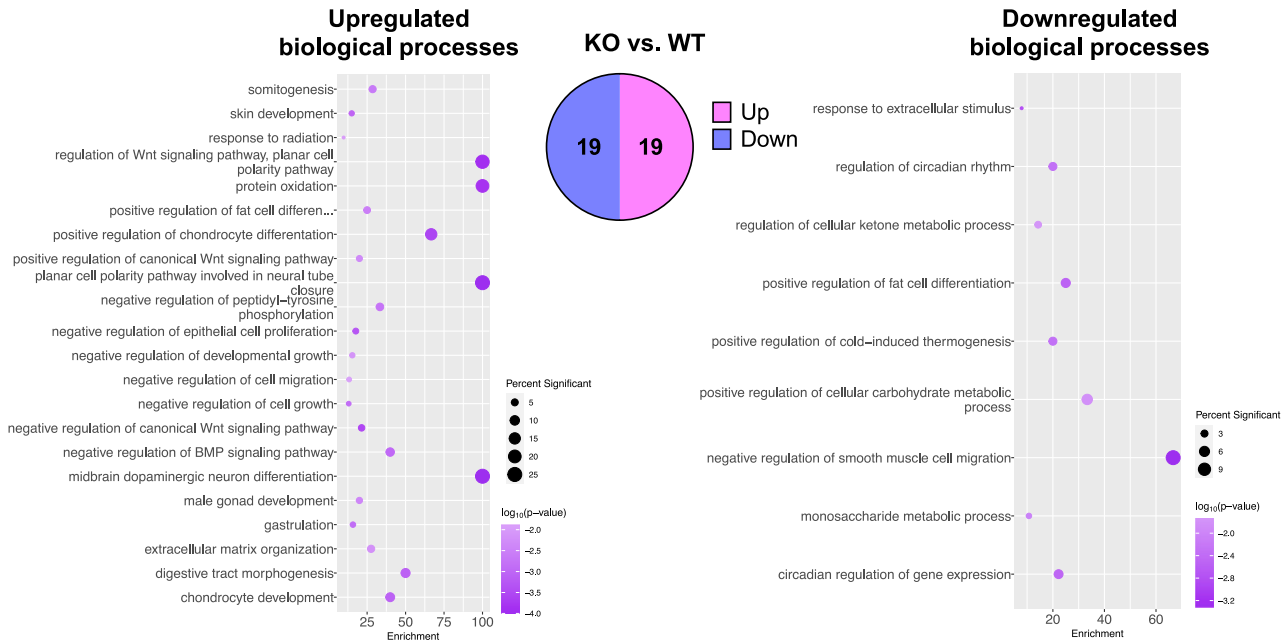

Figure 7. mRNAseq analysis in old KO versus WT atria

Transcript levels of 38 genes were significantly changed, where 19 genes were upregulated, and 19 were downregulated. The bubble plots show the biological processes associated with the differentially regulated genes. Enrichment indicates the ratio of genes with that GO term that are differentially expressed over what would be expected by chance. The size of the dots corresponds to the percentage of genes in that category that are differentially expressed, and the color corresponds to the p value on a log10 scale (more negative is more statistically significant).

pathways may contribute to differential modulation excitability in female versus male atria as well as in the atrial anatomy and can thus affect the dynamics of the arrhythmia.[53–56]

DISCUSSION

This work provides direct evidence that the PKCε/I_{KACh} pathway plays an important role in aging-mediated AF where constitutively active I_{KACh} contributes to AF perpetuation in the aging heart in a PKCε-dependent manner. This arrhythmogenic pathway has not been explored before in the aging heart. Our experiments showed that I_{KACh} is constitutively active in the old atria through a PKCε-dependent mechanism, where (1)- I_{KACh} is constitutively active in old atrial myocytes, and knocking out PKCε prevented the constitutive activity of this current, (2)- knocking out PKCε or blocking constitutively active I_{KACh} reduces atrial arrhythmogenesis in the old heart, and (3)- oxidative stress leads to the generation of a constitutively active I_{KACh} via PKCε activation. Our results correspond with epidemiological studies suggesting that clinically, AF prevalence increases with advanced age; in fact, aging is the single greatest risk factor for AF.[15–17]

Our data indicated sex-specific differences in AF inducibility in female versus male WT mice (Figure 1). Although sex-based differences in cardiac electrophysiology are known, they are still poorly understood.[2,57] For instance, atrial refractory period in response to rapid atrial pacing was significantly less in premenopausal compared with postmenopausal women and age-matched men, suggesting that estrogen and testosterone play important roles in modulating atrial repolarization.[58,59] This finding is consistent with the sex-differentiated enrichment of biological processes relevant to steroid pathways we found in the atria of female versus male WT mice (Figure 8). Sex-based differences in AF-related atrial remodeling is also observed in tissue samples from men and women with long-standing, persistent AF. A significantly higher degree of fibrotic remodeling was found in women,[60] which may contribute to higher incidence and recurrence rates of AF. In addition, sex-specific differences in immune system biology[53] have been found, as we have observed in our proteomics analysis. Such differences may lead to possible enhanced inflammatory responses in the female myocardium and subsequent modulation of fibrotic remodeling and arrhythmogenesis.[60] Consistent with these studies, our proteomics analysis (Figure 8) suggests the presence of sex-specific differences in immune response-related pathways. Sex is also suggested to modulate various AF risk factors. Obesity appears to increase the AF risk more in men than in women, coronary disease and

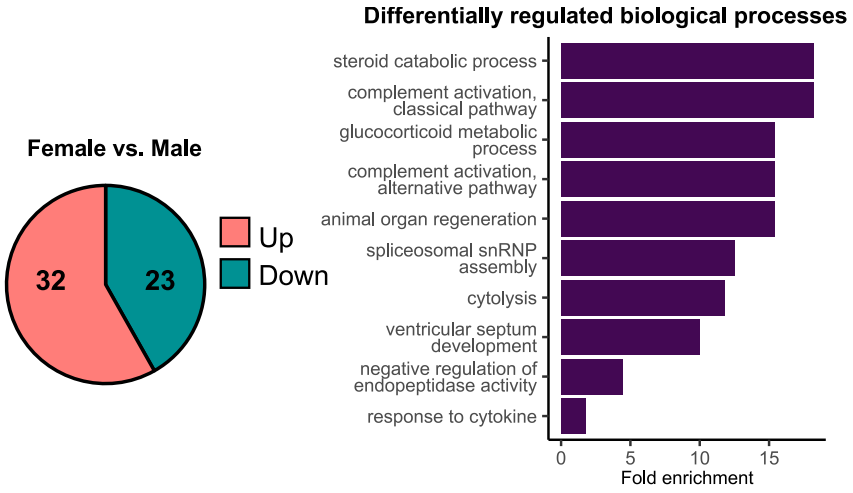

Figure 8. Proteomic analysis in WT female versus male atria

Protein levels of 55 genes were significantly different between the sexes, with 32 proteins increased and 23 proteins decreased in abundance in females compared to males. The bar graph shows enriched biological processes associated with the differentially regulated proteins. Enrichment indicates the ratio of genes with that GO term that are differentially expressed over what would be expected by chance.

sleep apnea have a higher prevalence in men with AF than women, while hypertension and heart failure with preserved ejection fraction are more prevalent in women with AF.[61] Overall, sex-based differences in arrhythmogenesis are multifaceted and complex, and thus, they are being actively investigated from the bench to the bedside. It is becoming clear that such differences may affect the clinical profile and even management of arrhythmias. However, a unified understanding of the sex-based differences in normal and abnormal cardiac excitability remains a work in progress, and this area deserves further study.

The generation and accumulation of ROS have been intimately linked to the cellular processes which underlie aging. By promoting oxidative damage to multiple subcellular and cellular structures, ROS have been suggested to promote the pathogenesis of AF by inducing structural and electrical remodeling including shortening of APD.[62–69] Our cellular studies support this interpretation and directly implicate PKCε as a key mediator of the relationship between oxidative stress and AF pathogenesis. Our data showed that ROS activate PKCε, induce its translocation to the cell membrane and increase I_{KACh}. Additionally, our patch clamp data showed that I_{KACh} is constitutively active in the old atrial myocytes via a mechanism that depends, at least in part, on PKCε. It has been proposed that in chronic AF, I_{KACh} is constitutively active and could be modulated by PKCε. Makary et al. showed that PKC isoforms differentially modulate I_{KACh}, with the conventional Ca^{2+}-dependent PKCα isoform inhibiting and the novel PKCε isoform enhancing activity.[41] Here, we provide evidence that aging-mediated AF inducibility and duration are reduced by abrogating constitutively active I_{KACh} via knocking out PKCε or by direct block with TPQ.

Studies have shown that ROS could also activate the ATP-sensitive inwardly rectifying potassium current (I_{KATP}).[70,71] I_{KATP} is another inwardly rectifying potassium current involved in AP repolarization and can mediate APD shortening and stabilization of arrhythmias and could thus be a target of PKCε. Additionally, oxidative stress could also lead to phosphorylation mediated decrease of the L type calcium current (LTCC).[72] Electrophysiological studies revealed that LTCC plays a crucial role in the electrical remodeling of AF,[73,74] where there is a reduction of LTCC,[75] contributing to APD shortening and possibly to AF initiation and perpetuation. Therefore, the LTCC and I_{KATP} can also be ionic mechanisms that are targets of PKCε and participate in promoting aging-mediated AF.

It has been demonstrated earlier by us and others that I_{KACh} block with TPQ or with chloroquine reduces the occurrence of persistent AF and restores sinus rhythm in animal models and in a patient with persistent AF.[76,77] It has been reported that the small molecules NTC-801,[78] and AZD2927,[79] were developed as selective inhibitors of I_{KACh}, which do not prolong the QT interval. However, these drugs failed to cardiovert paroxysmal AF and atrial flutter in patients. This could be due to the differences in the ionic bases of

paroxysmal and persistent AF. For instance, I_{KACh} is not constitutively active in patients with paroxysmal AF,[80] and the mechanisms of atrial flutter differ from those of persistent AF.[81]

LIMITATIONS OF THE STUDY

The pulmonary veins have been recognized as critically important sites of arrhythmogenic foci that trigger AF.[82–84] In the present study, we performed programmed electrical stimulation in the right atria to induce AF. Thus, our data may not reflect the spontaneous initiation mechanisms of aging-mediated AF in patients. We used a mouse model of PKCε global knockout which might result in confounders. For instance, the body weight of old KO mice is significantly smaller compared to old WT mice. Our RNA-seq data suggested that this could be due, in part, to the role that PKCε might play in metabolism and adipose tissue biology (Figure 7; Tables S1, S2, and S3). An inducible model of cardiac-specific PKCε knock down could be used in the future to assess, in a cardiac-specific manner, the role of PKCε and I_{KACh} in aging-mediated AF.

STAR★METHODS

Detailed methods are provided in the online version of this paper and include the following:

- KEY RESOURCES TABLE
- RESOURCE AVAILABILITY
  - Lead contact
  - Material availability
  - Data and code availability
- METHOD DETAILS
  - Animals
  - Single cell isolation
  - Cellular electrophysiology
  - In-vivo electrophysiology
  - Optical mapping studies
  - Total internal reflection fluorescence microscopy
  - RNAseq
  - Proteomics
- QUANTIFICATION AND STATISTICAL ANALYSIS

SUPPLEMENTAL INFORMATION

Supplemental information can be found online at https://doi.org/10.1016/j.isci.2022.105442.

ACKNOWLEDGMENTS

We are grateful to Dr. Douglas Bayliss, University of Virginia for providing the HEK cells stably transfected with Kir3.1 and Kir3.4. We acknowledge the contributions of the University of South Florida Genomics Program, including the sequencing core facility and USF Omics Hub for completion of this project. Funded in part, by NIH grant R01HL129136 to SFN and NIH grant R01HL059949-23 to DEL.

AUTHOR CONTRIBUTIONS

MC, DEL, JO, and SFN conceived experiments. MC, KDG, BC, AT, JG, ERW, JO, DEL, and SFN performed experiments and analyzed data. MC, KDG, JG, ERW, JO, DEL, and SFN wrote the manuscript. DEL, and SFN secured funding.

DECLARATION OF INTERESTS

The authors declare no competing interests.

Received: January 31, 2022
Revised: September 22, 2022
Accepted: October 20, 2022
Published: November 18, 2022

REFERENCES

1. Kannel, W.B., Abbott, R.D., Savage, D.D., and McNamara, P.M. (1982). Epidemiologic features of chronic atrial fibrillation: the Framingham study. N. Engl. J. Med. *306*, 1018–1022.

2. Lippi, G., Sanchis-Gomar, F., and Cervellin, G. (2021). Global epidemiology of atrial fibrillation: an increasing epidemic and public health challenge. Int. J. Stroke *16*, 217–221.

3. Bunch, T.J., Weiss, J.P., Crandall, B.G., May, H.T., Bair, T.L., Osborn, J.S., Anderson, J.L., Muhlestein, J.B., Horne, B.D., Lappe, D.L., and Day, J.D. (2010). Atrial fibrillation is independently associated with senile, vascular, and Alzheimer's dementia. Heart Rhythm *7*, 433–437.

4. Chen, L.Y., Lopez, F.L., Gottesman, R.F., Huxley, R.R., Agarwal, S.K., Loehr, L., Mosley, T., and Alonso, A. (2014). Atrial fibrillation and cognitive decline-the role of subclinical cerebral infarcts: the atherosclerosis risk in communities study. Stroke *45*, 2568–2574.

5. de Bruijn, R.F.A.G., Heeringa, J., Wolters, F.J., Franco, O.H., Stricker, B.H.C., Hofman, A., Koudstaal, P.J., and Ikram, M.A. (2015). Association between atrial fibrillation and dementia in the general population. JAMA Neurol. *72*, 1288–1294.

6. Dublin, S., Anderson, M.L., Haneuse, S.J., Heckbert, S.R., Crane, P.K., Breitner, J.C.S., McCormick, W., Bowen, J.D., Teri, L., McCurry, S.M., and Larson, E.B. (2011). Atrial fibrillation and risk of dementia: a prospective cohort study. J. Am. Geriatr. Soc. *59*, 1369–1375.

7. Elias, M.F., Sullivan, L.M., Elias, P.K., Vasan, R.S., D'Agostino, R.B., Seshadri, S., Au, R., Wolf, P.A., Benjamin, E.J., and Benjamin, E.J. (2006). Atrial fibrillation is associated with lower cognitive performance in the Framingham offspring men. J. Stroke Cerebrovasc. Dis. *15*, 214–222.

8. Forti, P., Maioli, F., Pisacane, N., Rietti, E., Montesi, F., and Ravaglia, G. (2007). Atrial fibrillation and risk of dementia in non-demented elderly subjects with and without mild cognitive impairment (MCI). Arch. Gerontol. Geriatr. *44*, 155–165.

9. Kalantarian, S., Stern, T.A., Mansour, M., and Ruskin, J.N. (2013). Cognitive impairment associated with atrial fibrillation: a meta-analysis. Ann. Intern. Med. *158*, 338–346.

10. Ott, A., Breteler, M.M., de Bruyne, M.C., van Harskamp, F., Grobbee, D.E., and Hofman, A. (1997). Atrial fibrillation and dementia in a population-based study. Stroke *28*, 316–321.

11. Thacker, E.L., McKnight, B., Psaty, B.M., Longstreth, W.T., Jr., Sitlani, C.M., Dublin, S., Arnold, A.M., Fitzpatrick, A.L., Gottesman, R.F., and Heckbert, S.R. (2013). Atrial fibrillation and cognitive decline: a longitudinal cohort study. Neurology *81*, 119–125.

12. Udompanich, S., Lip, G.Y.H., Apostolakis, S., and Lane, D.A. (2013). Atrial fibrillation as a risk factor for cognitive impairment: a semi-systematic review. QJM *106*, 795–802.

13. Wolf, P.A., Abbott, R.D., and Kannel, W.B. (1991). Atrial fibrillation as an independent risk factor for stroke: the Framingham Study. Stroke *22*, 983–988.

14. Chugh, S.S., Havmoeller, R., Narayanan, K., Singh, D., Rienstra, M., Benjamin, E.J., Gillum, R.F., Kim, Y.H., McAnulty, J.H., Jr., Zheng, Z.J., et al. (2014). Worldwide epidemiology of atrial fibrillation: a global burden of disease 2010 study. Circulation *129*, 837–847.

15. Kallergis, E.M., Goudis, C.A., and Vardas, P.E. (2014). Atrial fibrillation: a progressive atrial myopathy or a distinct disease? Int. J. Cardiol. *171*, 126–133.

16. Veasey, R.A., Sugihara, C., Sandhu, K., Dhillon, G., Freemantle, N., Furniss, S.S., and Sulke, A.N. (2015). The natural history of atrial fibrillation in patients with permanent pacemakers: is atrial fibrillation a progressive disease? J. Interv. Card. Electrophysiol. *44*, 23–30.

17. Andrade, J., Khairy, P., Dobrev, D., and Nattel, S. (2014). The clinical profile and pathophysiology of atrial fibrillation: relationships among clinical features, epidemiology, and mechanisms. Circ. Res. *114*, 1453–1468.

18. Kowey, P.R., Yan, G.X., Dimino, T.L., and Kocovic, D.Z. (2003). Overview of the management of atrial fibrillation: what is the current state of the art? J. Cardiovasc. Electrophysiol. *14*, 275–S280. discussion S280.

19. Dzeshka, M.S., Lip, G.Y.H., Snezhitskiy, V., and Shantsila, E. (2015). Cardiac fibrosis in patients with atrial fibrillation: mechanisms and clinical implications. J. Am. Coll. Cardiol. *66*, 943–959.

20. Wu, J., Xia, S., Kalionis, B., Wan, W., and Sun, T. (2014). The role of oxidative stress and inflammation in cardiovascular aging. BioMed Res. Int. *2014*, 615312.

21. Nattel, S., Burstein, B., and Dobrev, D. (2008). Atrial remodeling and atrial fibrillation: mechanisms and implications. Circ. Arrhythm. Electrophysiol. *1*, 62–73.

22. Elahi, M.M., Flatman, S., and Matata, B.M. (2008). Tracing the origins of postoperative atrial fibrillation: the concept of oxidative stress-mediated myocardial injury phenomenon. Eur. J. Cardiovasc. Prev. Rehabil. *15*, 735–741.

23. Chang, J.P., Chen, M.C., Liu, W.H., Yang, C.H., Chen, C.J., Chen, Y.L., Pan, K.L., Tsai, T.H., and Chang, H.W. (2011). Atrial myocardial nox2 containing NADPH oxidase activity contribution to oxidative stress in mitral regurgitation: potential mechanism for atrial remodeling. Cardiovasc.Pathol. *20*, 99–106.

24. Kim, Y.M., Guzik, T.J., Zhang, Y.H., Zhang, M.H., Kattach, H., Ratnatunga, C., Pillai, R., Channon, K.M., and Casadei, B. (2005). A myocardial Nox2 containing NAD(P)H oxidase contributes to oxidative stress in human atrial fibrillation. Circ. Res. *97*, 629–636.

25. Kim, Y.M., Kattach, H., Ratnatunga, C., Pillai, R., Channon, K.M., and Casadei, B. (2008). Association of atrial nicotinamide adenine dinucleotide phosphate oxidase activity with the development of atrial fibrillation after cardiac surgery. J. Am. Coll. Cardiol. *51*, 68–74.

26. Zhang, J., Youn, J.Y., Kim, A.Y., Ramirez, R.J., Gao, L., Ngo, D., Chen, P., Scovotti, J., Mahajan, A., and Cai, H. (2012). NOX4-Dependent hydrogen peroxide overproduction in human atrial fibrillation and HL-1 atrial cells: relationship to hypertension. Front. Physiol. *3*, 140.

27. Cha, T.J., Ehrlich, J.R., Chartier, D., Qi, X.Y., Xiao, L., and Nattel, S. (2006). Kir3-based inward rectifier potassium current: potential role in atrial tachycardia remodeling effects on atrial repolarization and arrhythmias. Circulation *113*, 1730–1737.

28. Dobrev, D., Graf, E., Wettwer, E., Himmel, H.M., Hála, O., Doerfel, C., Christ, T., Schüler, S., and Ravens, U. (2001). Molecular basis of downregulation of G-protein-coupled inward rectifying K(+) current (I(K, ACh) in chronic human atrial fibrillation: decrease in GIRK4 mRNA correlates with reduced I(K, ACh) and muscarinic receptor-mediated shortening of action potentials. Circulation *104*, 2551–2557.

29. Dobrev, D., Friedrich, A., Voigt, N., Jost, N., Wettwer, E., Christ, T., Knaut, M., and Ravens, U. (2005). The G protein-gated potassium current I(K, ACh) is constitutively active in patients with chronic atrial fibrillation. Circulation *112*, 3697–3706.

30. Sridhar, A., Nishijima, Y., Terentyev, D., Khan, M., Terentyeva, R., Hamlin, R.L., Nakayama, T., Gyorke, S., Cardounel, A.J., and Carnes, C.A. (2009). Chronic heart failure and the substrate for atrial fibrillation. Cardiovasc. Res. *84*, 227–236.

31. Li, D., Melnyk, P., Feng, J., Wang, Z., Petrecca, K., Shrier, A., and Nattel, S. (2000). Effects of experimental heart failure on atrial cellular and ionic electrophysiology. Circulation *101*, 2631–2638.

32. Kubo, Y., Reuveny, E., Slesinger, P.A., Jan, Y.N., and Jan, L.Y. (1993). Primary structure and functional expression of a rat G-protein-coupled muscarinic potassium channel. Nature *364*, 802–806.

33. Dascal, N., Schreibmayer, W., Lim, N.F., Wang, W., Chavkin, C., DiMagno, L., Labarca, C., Kieffer, B.L., Gaveriaux-Ruff, C., Trollinger, D., et al. (1993). Atrial G protein-activated K+ channel: expression cloning and molecular properties. Proc. Natl. Acad. Sci. USA *90*, 10235–10239.

34. Krapivinsky, G., Gordon, E.A., Wickman, K., Velimirović, B., Krapivinsky, L., and Clapham, D.E. (1995). The G-protein-gated atrial K+ channel IKACh is a heteromultimer of two

inwardly rectifying K(+)-channel proteins. Nature *374*, 135–141.

35. Hibino, H., Inanobe, A., Furutani, K., Murakami, S., Findlay, I., and Kurachi, Y. (2010). Inwardly rectifying potassium channels: their structure, function, and physiological roles. Physiol. Rev. *90*, 291–366.

36. Whorton, M.R., and MacKinnon, R. (2011). Crystal structure of the mammalian GIRK2 K+ channel and gating regulation by G proteins, PIP2, and sodium. Cell *147*, 199–208.

37. Logothetis, D.E., Kurachi, Y., Galper, J., Neer, E.J., and Clapham, D.E. (1987). The beta gamma subunits of GTP-binding proteins activate the muscarinic K+ channel in heart. Nature *325*, 321–326.

38. Wickman, K., and Clapham, D.E. (1995). Ion channel regulation by G proteins. Physiol. Rev. *75*, 865–885.

39. Wickman, K., Krapivinsky, G., Corey, S., Kennedy, M., Nemec, J., Medina, I., and Clapham, D.E. (1999). Structure, G protein activation, and functional relevance of the cardiac G protein-gated K+ channel, IKACh. Ann. N. Y. Acad. Sci. *868*, 386–398.

40. Nattel, S., Burstein, B., and Dobrev, D. (2009). In Cardiac electrophysiology: From cell to bedside, Zipes. and Jalife., eds. (Elsevier), pp. 453–465.

41. Makary, S., Voigt, N., Maguy, A., Wakili, R., Nishida, K., Harada, M., Dobrev, D., and Nattel, S. (2011). Differential protein kinase C isoform regulation and increased constitutive activity of acetylcholine-regulated potassium channels in atrial remodeling. Circ. Res. *109*, 1031–1043.

42. Voigt, N., Maguy, A., Yeh, Y.H., Qi, X., Ravens, U., Dobrev, D., and Nattel, S. (2008). Changes in I K, ACh single-channel activity with atrial tachycardia remodelling in canine atrial cardiomyocytes. Cardiovasc. Res. *77*, 35–43.

43. Voigt, N., Makary, S., Nattel, S., and Dobrev, D. (2010). Voltage-clamp-based methods for the detection of constitutively active acetylcholine-gated I(K, ACh) channels in the diseased heart. Methods Enzymol. *484*, 653–675.

44. Ferreira, J.C.B., Mochly-Rosen, D., and Boutjdir, M. (2012). Regulation of cardiac excitability by protein kinase C isozymes. Front. Biosci. *4*, 532–546.

45. Igumenova, T.I. (2015). Dynamics and membrane interactions of protein kinase C. Biochemistry *54*, 4953–4968.

46. Yu, H., Yang, Z., Pan, S., Yang, Y., Tian, J., Wang, L., and Sun, W. (2015). Hypoxic preconditioning promotes the translocation of protein kinase C epsilon binding with caveolin-3 at cell membrane not mitochondrial in rat heart. Cell Cycle *14*, 3557–3565.

47. Jung, Y.S., Ryu, B.R., Lee, B.K., Mook-Jung, I., Kim, S.U., Lee, S.H., Baik, E.J., and Moon, C.H. (2004). Role for PKC-epsilon in neuronal death induced by oxidative stress. Biochem. Biophys. Res. Commun. *320*, 789–794.

48. Yoo, S., Pfenniger, A., Hoffman, J., Zhang, W., Ng, J., Burrell, A., Johnson, D.A., Gussak, G., Waugh, T., Bull, S., et al. (2020). Attenuation of oxidative injury with targeted expression of NADPH oxidase 2 short hairpin RNA prevents onset and maintenance of electrical remodeling in the canine atrium: a novel gene therapy approach to atrial fibrillation. Circulation *142*, 1261–1278.

49. Jin, W., and Lu, Z. (1998). A novel high-affinity inhibitor for inward-rectifier K+ channels. Biochemistry *37*, 13291–13299.

50. Hashimoto, N., Yamashita, T., and Tsuruzoe, N. (2006). Tertiapin, a selective IKACh blocker, terminates atrial fibrillation with selective atrial effective refractory period prolongation. Pharmacol. Res. *54*, 136–141.

51. Steinberg, S.F. (2015). Mechanisms for redox-regulation of protein kinase C. Front.Pharmacol. *6*, 128.

52. Vyas, V., and Lambiase, P. (2019). Obesity and atrial fibrillation: epidemiology, pathophysiology and novel therapeutic opportunities. Arrhythm. Electrophysiol. Rev. *8*, 28–36.

53. Beale, A.L., Meyer, P., Marwick, T.H., Lam, C.S.P., and Kaye, D.M. (2018). Sex differences in cardiovascular pathophysiology: why women are overrepresented in heart failure with preserved ejection fraction. Circulation *138*, 198–205.

54. Chang, Y.T., Chen, Y.L., and Kang, H.Y. (2021). Revealing the influences of sex hormones and sex differences in atrial fibrillation and vascular cognitive impairment. Int. J. Mol. Sci. *22*, 8776.

55. Schulze-Bahr, E., Kirchhof, P., Eckardt, L., Bertrand, J., and Breithardt, G. (2005). Gender differences in cardiac arrhythmias. Herz *30*, 390–400.

56. Villareal, R.P., Woodruff, A.L., and Massumi, A. (2001). Gender and cardiac arrhythmias. Tex. Heart Inst. J. *28*, 265–275.

57. Johansson, C., Dahlqvist, E., Andersson, J., Jansson, J.H., and Johansson, L. (2017). Incidence, type of atrial fibrillation and risk factors for stroke: a population-based cohort study. Clin. Epidemiol. *9*, 53–62.

58. Pothineni, N.V., and Vallurupalli, S. (2018). Gender and atrial fibrillation: differences and disparities. US Cardiol. *12*, 103–106.

59. Bidoggia, H., Maciel, J.P., Capalozza, N., Mosca, S., Blaksley, E.J., Valverde, E., Bertran, G., Arini, P., Biagetti, M.O., and Quinteiro, R.A. (2000). Sex differences on the electrocardiographic pattern of cardiac repolarization: possible role of testosterone. Am. Heart J. *140*, 678–683.

60. Li, Z., Wang, Z., Yin, Z., Zhang, Y., Xue, X., Han, J., Zhu, Y., Zhang, J., Emmert, M.Y., and Wang, H. (2017). Gender differences in fibrosis remodeling in patients with long-standing persistent atrial fibrillation. Oncotarget *8*, 53714–53729.

61. Piccini, J.P., Simon, D.N., Steinberg, B.A., Thomas, L., Allen, L.A., Fonarow, G.C., Gersh, B., Hylek, E., Kowey, P.R., Reiffel, J.A., et al. (2016). Differences in clinical and functional outcomes of atrial fibrillation in women and men: two-year results from the ORBIT-AF registry. JAMA Cardiol. *1*, 282–291.

62. Lin, Y.K., Lin, F.Z., Chen, Y.C., Cheng, C.C., Lin, C.I., Chen, Y.J., and Chen, S.A. (2010). Oxidative stress on pulmonary vein and left atrium arrhythmogenesis. Circ. J. *74*, 1547–1556.

63. Goldhaber, J.I. (1996). Free radicals enhance Na+/Ca2+ exchange in ventricular myocytes. Am. J. Physiol. *271*, 823–833.

64. Morris, T.E., and Sulakhe, P.V. (1997). Sarcoplasmic reticulum Ca(2+)-pump dysfunction in rat cardiomyocytes briefly exposed to hydroxyl radicals. Free Radic. Biol. Med. *22*, 37–47.

65. Zissimopoulos, S., Docrat, N., and Lai, F.A. (2007). Redox sensitivity of the ryanodine receptor interaction with FK506-binding protein. J. Biol. Chem. *282*, 6976–6983.

66. Anzai, K., Ogawa, K., Ozawa, T., and Yamamoto, H. (2000). Oxidative modification of ion channel activity of ryanodine receptor. Antioxid. Redox Signal. *2*, 35–40.

67. Goldhaber, J.I., and Liu, E. (1994). Excitation-contraction coupling in single Guinea-pig ventricular myocytes exposed to hydrogen peroxide. J. Physiol. *477*, 135–147.

68. Hudasek, K., Brown, S.T., and Fearon, I.M. (2004). H2O2 regulates recombinant Ca2+ channel alpha1C subunits but does not mediate their sensitivity to acute hypoxia. Biochem.Biophys. Res. Commun. *318*, 135–141.

69. Guo, J., Giles, W.R., and Ward, C.A. (2000). Effect of hydrogen peroxide on the membrane currents of sinoatrial node cells from rabbit heart. Am. J. Physiol. Heart Circ. Physiol. *279*, 992–999.

70. Ardehali, H., and O'Rourke, B. (2005). Mitochondrial K(ATP) channels in cell survival and death. J. Mol. Cell. Cardiol. *39*, 7–16.

71. Mayanagi, K., Gáspár, T., Katakam, P.V.G., Kis, B., and Busija, D.W. (2007). The mitochondrial K(ATP) channel opener BMS-191095 reduces neuronal damage after transient focal cerebral ischemia in rats. J. Cereb. Blood Flow Metab. *27*, 348–355.

72. Hool, L.C. (2008). Evidence for the regulation of L-type Ca2+ channels in the heart by reactive oxygen species: mechanism for mediating pathology. Clin. Exp. Pharmacol. Physiol. *35*, 229–234.

73. Yue, L., Feng, J., Gaspo, R., Li, G.R., Wang, Z., and Nattel, S. (1997). Ionic remodeling underlying action potential changes in a canine model of atrial fibrillation. Circ. Res. *81*, 512–525.

74. Bosch, R.F., Zeng, X., Grammer, J.B., Popovic, K., Mewis, C., and Kühlkamp, V. (1999). Ionic mechanisms of electrical remodeling in human atrial fibrillation. Cardiovasc. Res. *44*, 121–131.

75. Van Wagoner, D.R., Pond, A.L., Lamorgese, M., Rossie, S.S., McCarthy, P.M., and Nerbonne, J.M. (1999). Atrial L-type Ca2+ currents and human atrial fibrillation. Circ. Res. *85*, 428–436.

76. Tobón, C., Palacio, L.C., Chidipi, B., Slough, D.P., Tran, T., Tran, N., Reiser, M., Lin, Y.S., Herweg, B., Sayad, D., et al. (2019). The antimalarial chloroquine reduces the burden of persistent atrial fibrillation. Front. Pharmacol. *10*, 1392.

77. Takemoto, Y., Slough, D.P., Meinke, G., Katnik, C., Graziano, Z.A., Chidipi, B., Reiser, M., Alhadidy, M.M., Ramirez, R., Salvador-Montañés, O., et al. (2018). Structural basis for the antiarrhythmic blockade of a potassium channel with a small molecule. FASEB J. *32*, 1778–1793.

78. Podd, S.J., Freemantle, N., Furniss, S.S., and Sulke, N. (2016). First clinical trial of specific IKACh blocker shows no reduction in atrial fibrillation burden in patients with paroxysmal atrial fibrillation: pacemaker assessment of BMS 914392 in patients with paroxysmal atrial fibrillation. Europace *18*, 340–346.

79. Walfridsson, H., Anfinsen, O.G., Berggren, A., Frison, L., Jensen, S., Linhardt, G., Nordkam, A.C., Sundqvist, M., and Carlsson, L. (2015). Is the acetylcholine-regulated inwardly rectifying potassium current a viable antiarrhythmic target? Translational discrepancies of AZD2927 and A7071 in dogs and humans. Europace *17*, 473–482.

80. Voigt, N., Friedrich, A., Bock, M., Wettwer, E., Christ, T., Knaut, M., Strasser, R.H., Ravens, U., and Dobrev, D. (2007). Differential phosphorylation-dependent regulation of constitutively active and muscarinic receptor-activated Ik, ACh channels in patients with chronic atrial fibrillation. Cardiovasc. Res. *74*, 426–437.

81. Olshansky, B. (2004). Combining ablation of atrial fibrillation with ablation of atrial flutter: are we there yet? J. Am. Coll. Cardiol. *43*, 2063–2065.

82. Steiner, I., Hájková, P., Kvasnicka, J., and Kholová, I. (2005). Pulmonary veins and atrial fibrillation: a pathological study of 100 hearts. Cesk.Patol. *41*, 124–131.

83. Steiner, I., Hájková, P., Kvasnicka, J., and Kholová, I. (2006). Myocardial sleeves of pulmonary veins and atrial fibrillation: a postmortem histopathological study of 100 subjects. Virchows Arch. *449*, 88–95.

84. Kholová, I., and Kautzner, J. (2003). Anatomic characteristics of extensions of atrial myocardium into the pulmonary veins in subjects with and without atrial fibrillation. Pacing Clin. Electrophysiol. *26*, 1348–1355.

85. Verheule, S., Sato, T., Everett, T., 4th, Engle, S.K., Otten, D., Rubart-von der Lohe, M., Nakajima, H.O., Nakajima, H., Field, L.J., and Olgin, J.E. (2004). Increased vulnerability to atrial fibrillation in transgenic mice with selective atrial fibrosis caused by overexpression of TGF-beta1. Circ. Res. *94*, 1458–1465.

86. Noujaim, S.F., Pandit, S.V., Berenfeld, O., Vikstrom, K., Cerrone, M., Mironov, S., Zugermayr, M., Lopatin, A.N., and Jalife, J. (2007). Up-regulation of the inward rectifier K+ current (I K1) in the mouse heart accelerates and stabilizes rotors. J. Physiol. *578*, 315–326.

87. Gray, R.A., Jalife, J., Panfilov, A., Baxter, W.T., Cabo, C., Davidenko, J.M., and Pertsov, A.M. (1995). Nonstationary vortexlike reentrant activity as a mechanism of polymorphic ventricular tachycardia in the isolated rabbit heart. Circulation *91*, 2454–2469.

88. Sarmast, F., Kolli, A., Zaitsev, A., Parisian, K., Dhamoon, A.S., Guha, P.K., Warren, M., Anumonwo, J.M.B., Taffet, S.M., Berenfeld, O., and Jalife, J. (2003). Cholinergic atrial fibrillation: I(K, ACh) gradients determine unequal left/right atrial frequencies and rotor dynamics. Cardiovasc. Res. *59*, 863–873.

89. Kim, D., Langmead, B., and Salzberg, S.L. (2015). HISAT: a fast spliced aligner with low memory requirements. Nat. Methods *12*, 357–360.

90. Liao, Y., Smyth, G.K., and Shi, W. (2014). featureCounts: an efficient general purpose program for assigning sequence reads to genomic features. Bioinformatics *30*, 923–930.

91. Robinson, M.D., McCarthy, D.J., and Smyth, G.K. (2010). edgeR: a Bioconductor package for differential expression analysis of digital gene expression data. Bioinformatics *26*, 139–140.

92. Robinson, M.D., and Oshlack, A. (2010). A scaling normalization method for differential expression analysis of RNA-seq data. Genome Biol. *11*, R25–R29.

93. Pagès, H., Falcon, S., and Li, N. (2018). AnnotationDbi: annotation database interface. R package version 1.44.0.

94. Carlson, M. (2018). org.Mm.eg.db: Genome wide annotation for Mouse. R package version 3.7.0.

95. Alexa, A., and Rahnenfuhrer, J. (2010). topGO: enrichment analysis for gene ontology. R package version 2.6.0.

96. Carlson, M. (2019). org.Mm.eg.db: Genome wide annotation for Mouse. R package version 3.10.0.

97. Rahnenfuhrer, A.A. (2019). topGO: enrichment analysis for gene ontology. R package version 2.38.1.

STAR★METHODS

KEY RESOURCES TABLE

REAGENT or RESOURCE	SOURCE	IDENTIFIER
Chemicals, peptides, and recombinant proteins		
Trypsin/Lys-C Mix	Promega	Cat#V5073
Collagenase A	Roche Diagnostics GmbH	Cat#10103578001 CAS#9001-12-1
Protease	Sigma-Aldrich	Cat#P5147 CAS#9036-06-0
Tertiapin-Q	Alomone Labs	Cat#STT-170 CAS#910044-56-3
Di-4-ANEEPPS	Sigma	CAT# D8064 CAS# 90134-00-2
(±)Blebbistatin	Abcam	Cat#ab120425 CAS#674289-55-5
RIPA buffer	Sigma-Aldrich	CAT#R0278
Protease and phosphatase inhibitor cocktail	Sigma-Aldrich	CAT#PPC1010
Critical commercial assays		
S-Trap micro columns	Protifi	CAT#C02-micro-10
RNeasy Mini kit	QIAGEN	CAT#74104
TruSeq RNA Library Prep Kit v2	Illumina	CAT#RS-122-2001
Deposited data		
RNA-seq (old KO vs. WT hearts)	This paper	GEO: GSE211472
Proteomics (WT female vs. male hearts)	This paper	MassIVE: MSV000090489
Experimental models: Cell lines		
HEK 293 Cells	Dr. Dougass Bayliss, University of Virginia	NA
Experimental models: Organisms/strains		
Mouse: B6.129S4-Prkce^{tm1Msg}/J	The Jackson Laboratory	Strain ID: 004,189 RRID: IMSR_JAX:004,189
Oligonucleotides		
PKC ε siRNA	Santa Cruz Biotechnology	Cat#sc-36251
Recombinant DNA		
mCherry-CRY2-PKCεCAT-HA	Dr. Diomedes E. Logothetis, Northeastern University	NA
Software and algorithms		
ImageJ	National Institute of Health, https://imagej.nih.gov/ij/	NA
Micromanager	University of California at San Francisco, https://micro-manager.org	NA
Multiclamp 700B amplifier	Molecular Devices	NA
Axon Digidata 1550B	Molecular Devices	NA
pClamp 10.6 PC software	Molecular Devices	NA
Clampfit 10.6	Molecular Devices	NA

(*Continued on next page*)

Continued

REAGENT or RESOURCE	SOURCE	IDENTIFIER
OriginPro 2018b software packages	OriginLab Corp	NA
Animal Bio Amp	AD Instruments	NA
PowerLab data acquisition system	AD Instruments	NA
Biopac System amplifier	Biopac Systems	NA
fastqc v0.11.5	Braham Institutte	NA
Multiqc v1.7	Multiqc.info	NA
hisat2 v2.1.0	Kim, D., B. Langmead, and S.L. Salzberg, HISAT: a fast spliced aligner with low memory requirements. Nature Methods, 2015. 12: p. 357.	NA
EdgeR v3.4.1	Robinson, M.D., D.J. McCarthy, and G.K. Smyth, edgeR: a Bioconductor package for differential expression analysis of digital gene expression data. Bioinformatics, 2010. 26(1): p. 139-40.	NA
AnnotationDbi	Pagès H, C.M., Falcon S, Li N, AnnotationDbi: Annotation Database Interface. R package version 1.44.0, 2018.	NA
Max quant 2.0.3.1	Maxquant.org	
org.Mm.eg.db R packages	Carlson, M., org.Mm.eg.db: Genomewide annotation for Mouse. R package version 3.10.0. R package version 3.10.0, 2019.	NA
The R package topGO version 2.48.0	Alexa A, Rahnenfuhrer J (2022). topGO: Enrichment Analysis for Gene Ontology. R package version 2.48.0.	NA

RESOURCE AVAILABILITY

Lead contact

Further information and requests for resources should be directed to and will be fulfilled by the lead contact, Dr. Sami F. Noujaim (snoujaim@usf.edu).

Material availability

The study did not generate new unique reagents.

Data and code availability

RNA seq data are available through the Gene Expression Omnibus: GSE211472, and the proteomics data are available through MassIVE: MSV000090489. Any additional information required to reanalyze the data reported in this paper is available from the lead contact upon request. This paper does not report original code.

METHOD DETAILS

Animals

All animal care procedures followed the NIH Guide for the Care and Use of Laboratory Animals and were approved by the Committee on Use and Care of Animals of the University of South Florida. Both male and female mice were used. The PKCε knockout (KO) mouse was purchased from the Jackson Laboratory. Experiments were performed in male and female young and old WT and KO animals. The average age of young animals was 3.9 $\pm$ 0.08 months and that of old mice was 20.9 $\pm$ 0.43 months. For euthanasia, CO_2 was used to induce loss of consciousness, and after loss of pinch reflex, swift cervical dislocation was performed, followed by rapid harvesting of the heart via thoracotomy. This method is consistent with the guidelines of the American Veterinary Medical Association.

Single cell isolation

Atrial myocytes were enzymatically dissociated from young and old WT and KO mice. In short, immediately after cardiac excision, the heart was cleaned, and the aorta was cannulated. The heart was then retrogradely perfused at 2 mL/min at 36 ± 0.5°C, for 3 min with Ca^{2+} free Tyrode solution (in mM): NaCl 137, KCl 5.4, HEPES 10, $MgCl_2$ 1, and glucose 10 (pH 7.3) until the effluent was clear of blood. Then the heart was perfused with the same solution containing collagenase 1 mg/mL collagenase Type A (Roche, Germany), and 0.08 mg/mL protease Type XIV (Sigma-Aldrich, USA) for 8 to 11 min, followed by Tyrode solution containing 0.2 mM $CaCl_2$ for 5 min. Single cells were then obtained by dissociation via gentle agitation of digested atrial tissues. Atrial myocytes suspensions were filtered through a nylon mesh, and cells were stored at room temperature in Tyrode solution. All solutions used for dissection and perfusion were continuously bubbled with 100% O_2.

Cellular electrophysiology

Atrial myocytes

The I_{KACh} current in atrial myocytes was measured with standard whole-cell voltage-clamp technique. The Multiclamp 700B (Molecular Devices) amplifier, an A/D converter (Digidata 1550B plus Hum Silencer, Molecular Devices), and the pClamp 10.6 PC software (Molecular Devices) were used for current acquisition. Clampfit 10.6 (pClamp, Molecular Devices) and OriginPro 2018b software packages (OriginLab Corp) were used for data analysis. Whole-cell measurements were performed at room temperature using borosilicate glass microelectrodes with tip resistances of 2.5–3 MΩ filled with pipette solution (in mM): KCl 140, $MgCl_2$ 1, HEPES 10, EGTA 5, Mg2ATP 5, and GTP 0.1, pH adjusted to 7.2 with KOH. Basal current was recorded by holding the atrial myocyte at −40 mV, followed by 1000 ms steps from −140 mV to +40 mV in 20 mV increments. The extracellular solution contained (in mM): NaCl 100, KCl 50, $MgCl_2$ 1, HEPES 5, and D-glucose 5.5, adjusted to pH 7.4. To measure the constitutively active I_{KACh} current in atrial cardiomyocytes, 100 nM Tertiapin-Q (TPQ, Alomone Labs) was applied to the extracellular solution.

HEK cells

HEK293 cells stably transfected with Kir3.1/Kir3.4 were a gift from Dr. Bayliss, University of Virginia. This cell line displays a basal I_{KACh}, without the need for muscarinic stimulation. I_{KACh} was recorded in these cells and the internal pipette solution contained (in mM): K-aspartate 100, NaCl 10, KCl 40, Mg-2ATP 5, EGTA 2, GTP-Tris 0.1, HEPES 10, pH 7.4. The bath solution contained (in mM): NaCl 90, KCl 50, $CaCl_2$ 1, $MgCl_2$ 2, HEPES 10, glucose 10, pH was adjusted to 7.4 with NaOH. The current was evoked in response to a ramp from −130 mV to 40 mV, from a holding potential of 0 mV, and subtracted from the residual current remaining after adding 1 mM $BaCl_2$ to the bath solution. In HEK293 cells stably expressing Kir3.1 and Kir3.4, SiRNA was used to silence PKCε (PKCε siRNA, Santa Cruz Biotechnology) according to the manufacturer's protocol.

In-vivo electrophysiology

Mice were anesthetized with 1.8% isoflurane. The ECG was recorded in Lead II configuration, and a 1.1 F octapolar Millar electrophysiology catheter, with an injection port for intracardiac delivery (Mikro-Tip catheter, ERP-801, Millar, USA), was placed in the right atrium through jugular access. The ECG and the intracardiac electrograms were simultaneously recorded using the Advanced Instruments platform. The cardiac signals were recorded via Animal Bio Amp (AD Instruments, USA) and digitized via the PowerLab data acquisition system (AD Instruments, USA). LabChart Pro 7.2 software (AD Instruments, USA) was used for acquisition and analysis of the cardiac electrical signals. To study AF inducibility and duration, intracardiac programmed electrical stimulation of the right atrium was performed via the catheter. The pacing protocol consisted of a 2-s burst, 2 x diastolic threshold, 2.5 ms pulse duration, increasing from 28 to 60 Hz in 2 Hz increments. AF was defined as a period of rapid irregular atrial rhythm lasting at least 2 s.[85] Animals showing AF episodes longer than 2 s were considered as inducible for AF. To test the effects of I_{KACh} block on AF, saline (50 μL) or TPQ (5 μM, in 50 μL saline) was injected through the catheter port.

Optical mapping studies

Optical mapping in the isolated Langendorff-perfused mouse heart was performed as described before.[86–88] Briefly, the excised hearts were rapidly cannulated and retrogradely perfused with normal Tyrode solution at 37°C. The heart was then placed in the well of a custom-made chamber maintained at 37°C. Optical mapping of the right atrial epicardial surface was carried out using a high-resolution CCD camera (1000 frames/s) and

Di-4-ANEEPPS (Sigma, St. Louis, MO, USA). The preparation was monitored using volume-conducted ECG in lead II configuration, recorded continuously with a Biopac System amplifier (DA100C; Biopac Systems, Inc., Goleta, CA, USA). Motion uncoupling was achieved with 7 μM blebbistatin (Abcam, USA). Action potential duration maps were generated as previously reported.[86–88]

Total internal reflection fluorescence microscopy

HEK293T cells were seeded on coverslips. 24 h later, cells were transfected with mCherry-CRY2-PKCεCAT-HA using polyethyleneimine (0.75 μg DNA: 3 μL PEI for 2 h). Total internal reflection fluorescence (TIRF) microscopy experiments were conducted the following day. mCherry was used as a proxy to detect the translocation of mCherry-CRY2-PKCεCAT-HA to the cell membrane. Cells were incubated with 100 μM H_2O_2 in a solution comprised of (in mM): NaCl 130, KCl 4, $MgCl_2$ 1.2, $CaCl_2$ 2, HEPES 10, pH was adjusted to 7.4 with NaOH. mCherry was excited with a 561 nm laser (Thor Labs) at 5, 15 and 30 min after treatment with H_2O_2. Images were captured at 5 s intervals to prevent bleaching and data were saved as separated stacks; the background was subtracted. Data were collected with Micromanager software and analyzed with ImageJ.

RNAseq

Atria from 3 WT old and 3 KO old male and female mice were isolated, flash-frozen then homogenized and lysed. mRNA was extracted from the tissue samples using the RNeasy kit from QIAGEN. Libraries were generated with TruSeq RNA Library Prep Kit v2 and sequencing was then performed on the USF Genomics Core NextSeq550 using 150 bp paired-end reads (75 bp each way). Sequencing-quality was measured using fastqc v0.11.5, and quality reports were aggregated using Multiqc v1.7. Resulting sequences were aligned against the *Mus musculus* reference genome GRCm38 (obtained from Ensembl; RefSeq ID: 5,034,988) using hisat2 v2.1.0[89] with RNA-strandedness set to paired-end. The gene expression-counts were estimated using FeatureCounts v1.5.0-p3.[90] Transcript-alignments were made against gene features annotated in *Mus_musculus.GRCm38.95.gtf* from Ensembl.

Differentially expressed genes in old KO versus old WT samples were determined using EdgeR v3.4.1.[91] Trimmed mean of M-values (TMM) normalization[92] was performed on all samples, and lowly expressed genes (having fewer than 10 counts-per-million reads (CPM) in any of the samples) were filtered out before analysis. Genes having a false discovery rate (FDR)-adjusted p value of less than or equal to 0.05 were considered differentially expressed.

Associated gene-ontology (GO) terms for all genes detected above threshold in the RNAseq data were extracted using the AnnotationDbi[93] and org.Mm.eg.db Bioconductor packages for R v3.5.[94] Differentially-expressed genes between KO and WT mice were then evaluated for GO-term enrichment against all detected genes using the weighted Fisher elimination hybrid test from topGO.[95]

Proteomics

Atrial samples were obtained from 3 young WT male and 3 young WT female mice. Samples were lysed in RIPA buffer and 1X protease inhibitor cocktail (Roche). SDS (5% final concentration) was added to 50 μg of the protein samples. All samples were prepped with S-Trap micro columns (Protifi) according to the manufacturer's protocol. For LC-MS analysis, the peptides were characterized using a Thermo Q-exactive-HF-X mass spectrometer coupled to a Thermo Easy nLC 1200. Samples were separated at 300 nL/min on an Acclaim PEPMAP 100 trap (75 μm, 2 cm, c18 3um, 100A) and a Thermo easyspray Column (75 μm, 25 cm, c18, 100A) using a standard 120-min gradient with an initial starting condition of 2% buffer B (0.1% formic acid in 90% Acetonitrile) and 98% buffer A (0.1% formic acid in water). The mass spectrometer was outfitted with a Thermo nanospray easy source with the following parameters: Spray voltage: 1.8, Capillary temperature: 250dC, Funnel RF level = 40. Parameters for data acquisition were as follows: for MS data the resolution was 60,000 with an AGC target of 3×10^6 and a max IT time of 50 ms, the range was set to 400–1600 *m/z*. MS/MS data was acquired with a resolution of 15,000, an AGC of 1×10^5, max IT of 50 ms, and the top 30 peaks were picked with an isolation window of 1.6 *m/z* with a dynamic execution of 25 s. Data were processed using Max quant 2.0.3.1 free software. A reviewed mouse database was downloaded from Uniprot and searched with the following parameters: a precursor mass tolerance of 10 ppm, and a fragment mass tolerance of 0.02 Da. FDR rate was set at 0.01, LFQ intensities were compared between samples for ID. LFQ intensities of proteins detected above threshold for at least two out of three samples for each sample-group were then assessed for differential abundance. Ratios comparing female versus males were generated and assessed for statistical significance using Welch's t-test. Absolute differences between female

and male abundances for each protein were calculated to determine direction of difference (positive numbers = higher in females, negative numbers = lower in females) and range over which to normalize for comparison between proteins (*Z* score). Abundance ratios were then normalized across all proteins such that 0 indicated no difference between the sexes, and the largest number indicated greatest difference. Proteins having a *Z* score > 1 and Welch's t-test p value < 0.05 were considered significant. The differentially abundant proteins were assessed for gene ontology enrichment against a background of all proteins detected above threshold for which the female/male ratio could be determined. Gene ontology annotations were obtained from the AnnotationDBI and org.Mm.eg.db R packages (version 1.56.2 and 3.14.0, respectively).[93,96] The R package topGO version 2.48.0 was used to calculate gene ontology enrichment using the weight01 algorithm and the Fisher exact test.[97] Gene ontology categories with a p value of less than or equal to 0.05 were considered enriched.

QUANTIFICATION AND STATISTICAL ANALYSIS

The data are expressed as mean ± SEM, or as boxplots (Median, 25th and 75th percentiles, minimum and maximum). Data normality was assessed with the Shapiro-Wilk test. For statistical analysis, Chi square, Student's *t* test, Mann Whitney Wilcoxon test, one-way ANOVA and linear mixed model were used as appropriate. Statistical significance was taken as $p < 0.05$.